Bilayer Interactions of Indolicidin, a Small Antimicrobial Peptide Rich in Tryptophan, Proline, and Basic Amino Acids

Alexey S. Ladokhin,*# Michael E. Selsted,# and Stephen H. White*
*Department of Physiology and Biophysics, University of California, Irvine, California 92697-4560, and #Department of Pathology, University of California, Irvine, California 92697-4800 USA

ABSTRACT Tryptophan, proline, and basic amino acids have all been implicated as being important in the assembly and structure of membrane proteins. Indolicidin, an antimicrobial 13-residue peptide-amide isolated from the cytoplasmic granules of bovine neutrophils, is highly enriched in these amino acids: five tryptophans, three prolines, three basic residues, and no acidic residues. Consistent with the likely importance of these amino acids in membrane protein assembly, indolicidin is known to be highly membrane-active and is believed to act by disruption of cell membranes. We have, therefore, examined the interactions of native indolicidin with large unilamellar vesicles (LUV) formed from palmitoyloleoylphosphatidylcholine (POPC), and palmitoyloleoylphosphatidylglycerol (POPG), in order to use it as a model system for studying membrane protein insertion and for evaluating the relative contributions of hydrophobic and electrostatic forces in peptide-bilayer interactions. Equilibrium dialysis measurements indicate that indolicidin binds strongly, but reversibly, to both neutral POPC and anionic POPG vesicles with free energies of transfer of -8.8 ± 0.2 and -11.5 ± 0.4 kcal/mol, respectively. The extremely strong partitioning into POPG vesicles necessitated the development of a new equilibrium dialysis method that is described in detail. Tryptophan fluorescence measurements show that indolicidin is located in the bilayer interface and that indole fluorescence is affected by the type of lipid used to form the LUVs. Circular dichroism (CD) measurements reveal unordered conformations in aqueous and bulk organic solutions and a somewhat more ordered, but not α-helical, conformation in SDS micelles and lipid bilayers. Fluorescence requenching measurements (Ladokhin et al. 1995. *Biophys. J.* 69:1964–1971) on vesicles loaded with the fluorophore/quencher pair 8-aminonapthalene-1,3,6 trisulfonic acid (ANTS)/*p*-xylene-*bis*-pyridinium bromide (DPX), show that indolicidin induces membrane permeabilization. For anionic POPG, leakage is graded with a high preference for the release of cationic DPX over anionic ANTS. For neutral POPC vesicles no such preference is observed. Leakage induction is more effective with POPG vesicles than with POPC vesicles, as judged by three quantitative measures that are developed in the Appendix.

INTRODUCTION

Indolicidin is a positively charged antimicrobial tridecapeptide-amide isolated from the cytoplasmic granules of bovine neutrophils (Selsted et al., 1992). Its primary structure is remarkable because of its high content of tryptophan (five residues), proline (three residues), and arginine (two residues):

Ile-Leu-Pro-Trp-Lys-Trp-Pro-Trp-Trp-Pro-Trp-Arg-Arg-Amide

The basis for its antimicrobial action is believed to be membrane disruption because aggregated indolicidin (concentrations >30 μM) causes lysis of red blood cells (Ahmad et al., 1995). Indolicidin's membrane-active nature, and its rich content of tryptophan, proline, and basic amino acids, make it an intriguing peptide for study because all of these amino acids have been implicated as important in the assembly and structure of membrane proteins (von Heijne, 1989; Williams and Deber, 1991; Wimley and White, 1993a; Schiffer et al., 1992).

As we demonstrate in this paper, indolicidin has a largely unordered conformation when free and when bound to bilayers. This makes it a good peptide for testing the additivity of single-residue hydrophobicity parameters which can only be done for peptides that form no secondary structure when bound (Wimley and White, 1996). Because indolicidin is simultaneously hydrophobic due to its tryptophan residues and charged due to its basic residues, its interactions with a broad range of lipids can be examined and compared. These features make indolicidin a useful model system for understanding the relative contributions of hydrophobic and electrostatic interactions in peptide-bilayer interactions. Other natural peptides, such as melittin (Dempsey, 1990; Sessa et al., 1969), can also be useful in this regard, but indolicidin's small size, its lack of secondary structure, and the relative ease with which variant peptides can be synthesized, make it especially useful. Furthermore, the five tryptophans provide a unique opportunity to examine the role of tryptophan in the insertion of proteins into

Received for publication 13 August 1996 and in final form 28 October 1996.

Address reprint requests to Dr. Stephen H. White, Dept. of Physiology and Biophysics, University of California School of Medicine-Irvine, Irvine, CA 92697-4560. Tel.: 714-824-7122; Fax: 714-824-8540; E-mail: shwhite@uci.edu.

Dr. Ladokhin's permanent address is Palladin Institute of Biochemistry, National Academy of Sciences of Ukraine, Kiev 252030, Ukraine.

The abbreviations used are: POPG: palmitoyloleoylphosphatidylglycerol. POPC: palmitoyloleoylphosphatidylcholine. LUV: extruded unilamellar vesicles of 100 nm diameter. ANTS: 8-aminonapthalene-1,3,6 trisulfonic acid. DPX: *p*-xylene-*bis*-pyridinium bromide. TOE: tryptophan octyl ester. HEPES: *N*-2-hydroxyethylpiperazine-*N'*-2-ethanesulfonic acid. EDTA: ethylenediamine-tetraacetic acid. CD: circular dichroism spectroscopy. SDS: sodium dodecyl sulfate. Triton: Triton X-100 (Union Carbide Chemicals and Plastics Co.), a polydisperse octylphenylpolyoxyethylene surfactant.

0006-3495/97/02/794/12 $2.00

membranes (Wimley and White, 1993a). As a first step toward understanding its possible interactions with natural membranes and toward using it as a model for studying general peptide-bilayer interactions and membrane protein insertion, we have examined the interactions of native indolicidin with lipid bilayers formed from neutral and anionic lipids. Our goals were to characterize its binding and conformation and to examine its effect on bilayer structure through its ability to induce leakage of vesicle contents. A preliminary account of this work has been presented (Ladokhin et al., 1996).

We find strong indolicidin partitioning into unilamellar vesicles (LUV) formed from either neutral POPC or anionic POPG. The peptide at relatively low concentrations induces leakage of the fluorophore/quencher pair ANTS/DPX from both systems, but by apparently different mechanisms. The application of the fluorescence requenching technique (Ladokhin et al., 1995) indicates that the leakage from POPG vesicles is graded with a strong preference for DPX release. Requenching data for POPC vesicles are consistent with several release mechanisms, none of which, however, has a preference for DPX. Because the kinetics of indolicidin-induced leakage are complex and affected by lipid composition, we define in the Appendix three quantitative measures of the effectiveness of release. These measures indicate that the overall induction of leakage from POPG vesicles is more efficient than from POPC vesicles. This is consistent with differences in the organization of leakage pathways in two lipid systems.

Bilayer partitioning increases the quantum yield of indolicidin's fluorescence and induces a blue shift in the spectrum. The blue shift is greater and the quantum yield lower for POPG than for POPC. Similar spectral differences are seen for the well-characterized model compound tryptophan octyl ester (TOE) (Ladokhin and Holloway, 1995b). This suggests that the fluorescent tryptophan(s) of indolicidin are located in the vicinity of the bilayer interface. Circular dichroism (CD) spectroscopy indicates that indolicidin adopts an unordered conformation in both aqueous and organic (trifluoroethanol, methanol) solutions. In SDS micelles, indolicidin adopts a slightly more ordered (but not an α-helical) structure and, in addition, exhibits a strong negative band at 230 nm, attributed to tryptophans with restricted conformations. CD spectra of indolicidin in POPC and POPG bilayers are very similar to each other and to those observed using SDS micelles.

MATERIALS AND METHODS

Materials

Lipids were obtained from Avanti Polar-Lipids (Birmingham, AL), ANTS and DPX from Molecular Probes (Eugene, OR), and tryptophan, TOE, and FD-4 from Sigma (St. Louis, MO). Indolicidin was purified from bovine neutrophils (Selsted et al., 1992) or was synthesized by solid-phase techniques according to the methods of Van Abel et al. (1995). Melittin was a gift of Dr. E. Habermann. The buffer solution (pH 7.0) used for most experiments contained 10 mM HEPES, 50 mM KCl, 1 mM EDTA, and 3 mM NaN_3. For the melittin experiments, 5 mM EDTA was used. To reduce the UV absorbance in CD measurements, a 50-mM potassium phosphate buffer (pH = 7.0) was used instead of HEPES. The concentration of indolicidin was never >30 μM to avoid aggregation.

Preparation of vesicles

Large unilamellar vesicles (LUV) of ~0.1 μm diameter were formed by extrusion under N_2 pressure through Nucleopore polycarbonate membranes, using the method of Mayer et al. (1986). To prepare LUV with entrapped ANTS and DPX, the lipid was suspended in buffer containing the solute and then frozen and thawed 20 times before extrusion. Lipid solutions were prepared at 100 mM to maximize entrapment. The total KCl concentration in ANTS- and DPX-containing vesicles was adjusted so that the entrapped solutions had the same osmolarity as the external 50-mM KCl buffer. Unencapsulated ANTS and DPX were separated from encapsulated material using Sephadex G-100 packed in a 2.5-ml Pasteur pipette. A detailed description of the procedure has been presented by Wimley et al. (1994).

Partition coefficients

Partition coefficients are often determined by measuring the change in some optical property, such as fluorescence, as a peptide solution is titrated with lipid vesicles. The primary data then consist of titration curves from which partition coefficients are determined from the change in the optical property. A difficulty with this approach is that the amount of peptide bound per lipid changes dramatically with the titration, which makes it difficult to detect concentration-dependent changes in partitioning. This particular problem can be overcome by working at very low peptide concentrations, but then the changes in the optical property can be difficult to quantitate. To avoid these problems, we use mole-fraction partition coefficients determined using equilibrium dialysis and quantitative reverse-phase HPLC as described in detail elsewhere (Wimley and White, 1993b). The primary data in this case consist only of measurements of the concentrations of lipid and peptide in the two halves of a dialysis cell at equilibrium. Briefly, a suspension of lipid vesicles was placed in one-half of an equilibrium dialysis cell (Spectrum Medical Industries, Houston, TX) that was separated from the other half by a semi-permeable cellulose membrane. A solution of peptide was placed in the other half-cell. With constant rotation of the cells in a thermostat, indolicidin equilibrated across the membrane in <12 h. We generally allowed the system to equilibrate for 24 or more hours at 25°C. The mole-fraction partition coefficient (K_x) is given by

$$K_x = \frac{[P]_{bil}/([L] + [P]_{bil})}{[P]_{water}/([W] + [P]_{water})} \quad (1)$$

where $[P]_{bil}$ and $[P]_{water}$ are the bulk molar concentrations of peptide attributable to peptide in the bilayer and water phases, respectively (Wimley and White, 1993b). In the vesicle-containing half-cell, $[P]_{total} = [P]_{bil} + [P]_{water}$. $[L]$ and $[W]$ are the molar concentrations of lipid and water. Equation 1 assumes that all lipid is accessible to the peptide. If only the outer leaflet of the bilayer is accessible, then one should replace $[L]$ by $[L]/2$. Unfortunately, there is no way to establish with certainty the transbilayer distribution of the peptide. The practical consequence of this uncertainty is that the *absolute* value of the free energy of transfer is uncertain (see below). Our experience is that most membrane-active peptides induce some leakage from vesicles, which suggests significant perturbation of the bilayer that could lead to transbilayer redistribution. We have chosen to use $[L]$ rather than $[L]/2$ as standard practice.

It is always true in our measurements that $[W] = 55.3\ M \gg [P]_{water}$, and generally one keeps the concentration of peptide in the bilayer low to avoid anti-cooperative behavior of charged peptides, so that $[L] \gg [P]_{bil}$.

Therefore, to high accuracy one may write

$$K_x = \frac{[P]_{bil}/[L]}{[P]_{water}/[W]} \quad (2)$$

There is an upper limit on the value of K_x that can be determined under the conditions of Eq. 2 because of the inherent conflict between low bilayer concentrations on the one hand and peptide detectability by HPLC on the other. Very strong partitioning requires that the lipid concentration be kept low so that the aqueous concentration of peptide does not drop below the level that can be measured accurately. However, it also requires low aqueous peptide concentrations to keep the bilayer concentration of peptide in the dilute range. The end result is that HPLC instrumental sensitivity prevents determination of values of K_x that are greater than a particular value that depends on the detectability of a given peptide. The upper limit for indolicidin is 3×10^7.

The partitioning of indolicidin into POPG vesicles was so strong that these limitations were exceeded. No free peptide could be detected over the range of lipid concentrations (0.05–5 mM) normally used for POPC partitioning. We therefore developed a new procedure for determining the partitioning into POPG vesicles. Instead of equilibrating POPG vesicles against a simple peptide solution, we equilibrated them against a solution containing POPC vesicles whose peptide partition coefficient K_x^{POPC} had been determined using the standard scheme. Because the unbound indolicidin concentrations $[P]_{water}$ must be equal in the half-cells at equilibrium and are known from measurements with POPC, one may write

$$K_x^{POPG} = K_x^{POPC} \frac{([P]_{POPG} - [P]_{water})/[POPG]}{([P]_{POPC} - [P]_{water})/[POPC]} \quad (3a)$$

where the concentration of peptide in the buffer is calculated from

$$[P]_{water} = [P]_{POPC}\left(\frac{[W]}{K_x^{POPC}[POPC] + [W]}\right) \quad (3b)$$

$[P]_{POPC}$ and $[P]_{POPG}$ are the concentrations of peptide in the POPC and POPG half-cells, respectively. Manipulation of the lipid concentrations, $[POPC]$, and $[POPG]$, allows one to overcome the limitations of the standard scheme and thereby quantitate accurately strong partitioning. We found that these measurements did not depend on whether indolicidin was initially placed on the POPC or POPG side, indicating reversibility of binding. However, because of the low fraction of free peptide (<5%), the equilibration was slow. Therefore an equilibration time of 72 h was used for these measurements.

Free energies of transfer

Mole-fraction free energies of transfer (kcal/mol) were determined from the partition coefficients using $\Delta G = -RT \ln K_x^i$ where i = POPC or POPG. We have chosen to use total lipid concentration in K_x^i determinations as described above. If one wishes to assume that indolicidin does not penetrate the inner leaflet, one should add −0.41 kcal/mol to the ΔG values reported here.

Leakage experiments

A small volume (10–25 μl) of a concentrated stock solution of vesicles with entrapped ANTS/DPX was quickly added into 1 ml buffer containing peptide and immediately stirred. In some cases, the procedure was reversed: a concentrated peptide solution was added to a dilute vesicle suspension. For the quantitative analysis of leakage kinetics, only the former approach was used. Leakage assays were performed with a SPEX Fluorolog spectrofluorometer that was upgraded and interfaced to a computer by OLIS, Inc. (Jefferson, GA). The excitation and emission wavelengths were kept at 380 and 520 nm with slits of 20–40 nm to increase the signal. The contribution of light scattering was negligible in all cases. We limited the leakage study to peptide concentrations not higher than 30 μM because the aggregated form of the peptide appeared to interfere with the leakage assay, possibly due to binding of ANTS. Light scattering experiments (data not shown) suggest the formation of large aggregates at indolicidin concentrations >30 μM, which is consistent with result of Ahmad et al. (1995) reported for a somewhat different buffer system.

Fusion assay

Fusion was studied by a standard 7-nitro-benzoxadiazole-PE/rhodamine-PE fluorescence energy transfer method as described by Wimley et al. (1994) using an SLM-8100 fluorimeter (SLM/Aminco, Urbana, IL). Excitation and emission wavelengths were 468 nm and 535 nm, with slits of 2 nm and 8 nm, respectively. To reduce possible contributions from scattering, a polarizer transparent for horizontally polarized light was introduced into the emission path.

UV Fluorescence Measurements

Tryptophan fluorescence measurements were performed using the SLM-8100 spectrofluorometer. Polarizers in the magic-angle configuration were used to exclude artifacts associated with dynamic depolarization. Spectral measurements were performed at an excitation wavelength of 270 nm, with excitation and emission slits set to 4 nm. Averaged emission spectra were obtained from multiple scans (5–15) from 290 to 500 nm with a 1-nm increment. After the spectrum for the blank was subtracted, the spectrum was fitted to a log-normal distribution as described by Ladokhin et al. (1991) to obtain the position of the maximum and the area under the curve. The latter was used to calculate the relative quantum yield by comparing its value with the one for an aqueous solution of tryptophan. The intensity data were corrected for membrane scattering using tryptophan with the same concentration of lipid as in the peptide sample. Equilibrium dialysis partitioning experiments indicate that tryptophan does not bind to vesicles under our experimental conditions (Wimley and White, unpublished). The correction factor did not exceed 12%. All measurements were performed at 25°C.

Fluorescence anisotropy was determined from intensities measured at 350 nm (8-nm slits) with a vertical (V) and horizontal (H) position of the polarizer (first subscript) and analyzer (second subscript):

$$r = \frac{I_{VV} - G \cdot I_{VH}}{I_{VV} + 2G \cdot I_{VH}}$$

where the correction factor $G = I_{HV}/I_{HH}$ was determined by averaging a series of experiments. Samples for fluorescence measurements contained 2–5 μM indolicidin or TOE, and 0.6 mM lipid.

Circular dichroism and absorbance spectroscopy

CD measurements were performed using a Jasco-720 spectropolarimeter (Japan Spectroscopic Company, Tokyo, Japan). Normally, 50–250 scans were recorded between 185 and 260 nm. Samples contained 10–25 μM indolicidin and 1.1 mM lipid. A 1-mm optical path was used. UV absorbance was measured with a Cary 3E spectrophotometer (Varian Analytical Instruments, Sugar Land, TX). No smoothing of the data was performed.

Fluorescence requenching

The mechanism of leakage induction by indolicidin was determined by fluorescence requenching (Ladokhin et al., 1995; Wimley et al., 1994). Briefly, after partial leakage of vesicle contents (ANTS/DPX) has occurred, the vesicle solutions are titrated with DPX to determine the degree to which the dye molecules remaining in the vesicles are quenched. If the quenching inside, Q_{in}, does not change with the fraction of dye released,

f_{out}, the mechanism is all-or-none. For graded release, the quenching inside changes (Ladokhin et al., 1995) according to

$$Q_{in} = [(1 + K_d \cdot [DPX]_0 \cdot (1 - f_{out})^{\alpha}) \cdot (1 + K_a \cdot [DPX]_0 \cdot (1 - f_{out})^{\alpha})]^{-1} \quad (4)$$

The parameters K_d, K_a, and $[DPX]_0$ are defined below. The fraction f_{out}^{DPX} of DPX released is assumed to be related to the fraction $f_{out} \equiv f_{out}^{ANTS}$ of ANTS released according to

$$f_{out}^{DPX} = 1 - (1 - f_{out})^{\alpha} \quad (5)$$

which defines the preferential-release parameter α. For the simplest case of exponential leakage, α coincides with the ratio of kinetic rates of DPX and ANTS release.

The values for the quenching constants for the ANTS/DPX pair, K_d = 50 M^{-1} and K_a = 490 M^{-1}, were determined previously (Ladokhin et al., 1995). The initial concentration of DPX inside the vesicles, $[DPX]_0$, and the preferential release parameter, α, can be obtained by fitting the experimental data to Eq. 4, which can also be used to distinguish all-or-none from graded release. Values of $\alpha = 1$, < 1, and > 1 indicate, respectively, nonpreferential release of ANTS and DPX, preferential release of ANTS, and preferential release of DPX. All-or-none release is nonpreferential by definition, but mathematically it coincides with a limiting case of $\alpha = 0$ with Q_{in} becoming independent of f_{out} in Eq. 4. The derivation of Eq. 4 and details of the experimental determination of Q_{in} and f_{out} have been given elsewhere (Ladokhin et al., 1995). Nonlinear least-squares analyses and data simulations were performed with the software package Origin 3.5 (MicroCal, Inc., Northampton, MA).

Kinetic analysis

The fraction of dye released $f_{out}(t)$ as a function of the time t that elapsed after mixing of marker-loaded vesicles with indolicidin is described by

$$f_{out}(t) = A_0 + A_1 \cdot [1 - \exp(-k_1 t)] \quad (6)$$

where A_0, A_1, and k_1 are parameters determined by nonlinear-least-squares methods. Conversion of efflux of markers into fluorescence kinetics was performed as described by Ladokhin et al. (1995; also see Appendix for more details).

RESULTS

Partitioning of indolicidin into POPC and POPG vesicles

The primary data from the equilibrium dialysis measurements are summarized in Table 1. Note that a wide range of lipid and peptide concentrations have been used in order to be certain that the reported partition coefficient and free energy values are independent of the concentration of bound peptide. Partition coefficients and free energies of transfer were determined from these data as described in Methods. Indolicidin partitions strongly into POPC LUV (*square symbols*, Fig. 1) with a mole-fraction partition coefficient of $2.9 \pm 0.9 \times 10^6$, which yields a water-to-bilayer free energy of transfer $\Delta G = -8.8 \pm 0.2$ kcal/mol. The partition coefficient for POPG LUV (*triangles*, Fig. 1) was found to be $2.8 \pm 1.5 \times 10^8$ corresponding to $\Delta G = -11.5 \pm 0.4$ kcal/mol. Fig. 1 shows that these values are independent of peptide/lipid ratio $[P]_{bil}/[L]$ over a wide range of concentrations. At extremely high $[P]_{bil}/[L]$ ratios, however, partitioning decreases (*open symbols*), probably because of anticooperative effects due to electrostatic repulsion of peptide molecules. Note that the effect occurs at a higher $[P]_{bil}/[L]$ ratio for POPG than for POPC, presumably because of the lipid charge.

TABLE 1 Partitioning of indolicidin into POPC and POPG vesicles determined by equilibrium dialysis

	Left half-cell*			Right half-cell*		
	Lipid	Lipid (mM)#	Indolicidin (μM)§¶	Lipid	Lipid (mM)#	Indolicidin (μM)§‖
1	POPC	0.05	0.81	None		0.15
2	POPC	0.05	57	None		51
3	POPC	0.07	1.6	None		2.6
4	POPC	0.12	0.31	None		0.02
5	POPC	0.12	3.6	None		0.82
6	POPC	0.13	0.09	None		0.01
7	POPC	0.13	2.9	None		0.34
8	POPC	0.44	0.48	None		0.02
9	POPC	0.77	0.63	None		0.03
10	POPC	1.10	1.5	None		0.04
11	POPG	0.005	3.6	None		2.1
12	POPG	0.005	4.5	POPC	0.35	58
13	POPG	0.005	0.68	POPC	0.38	0.53
14	POPG	0.010	0.26	POPC	0.75	0.21
15	POPG	0.054	0.22	POPC	1.85	0.06

*Equilibrium dialyses apparatus is described by Wimley and White (1993b) and consists of two half-cells separated by a semipermeable membrane. The designations of half-cells as "left" or "right" is arbitrary.

#Lipid concentrations were determined by dilution of stock solutions for which concentrations were determined by a phosphate analysis. Experimental uncertainty in concentrations listed is $\pm 5\mu$M for POPC and $\pm 1\mu$M for POPG.

§Indolicidin concentrations were determined by HPLC as described by Wimley and White (1993b). Injection volumes varied from 0.05 to 1.0 ml. Experimental uncertainties are nominally $\pm 10\%$ (range: 3–30%).

¶Corresponds to $[P]_{bil} + [P]_{water}$ for use in Eq. 2 for rows 1–11 and $[P]_{POPG}$ for use in Eq. 3 for rows 12–15.

‖Corresponds to $[P]_{water}$ for use in Eq. 2 for rows 1–11 and to $[P]_{POPC}$ for use in Eq. 3 for rows 12–15.

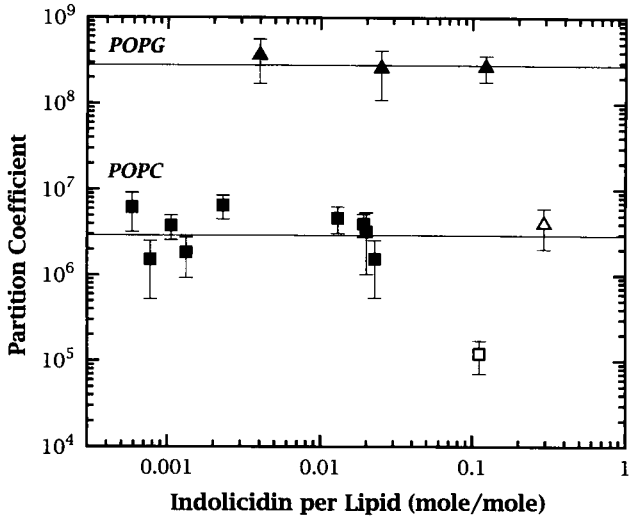

FIGURE 1 Partition coefficients as functions of the mole ratio of bound indolicidin to lipid for LUV formed from POPC (*squares*) or POPG (*triangles*). Horizontal lines correspond to error-weighted average values of 2.9×10^6 and 2.8×10^8 for POPC and POPG, respectively. Partition coefficients are independent of the peptide/lipid ratio over a broad range. At very high ratios (*open symbols*), indolicidin partitions to a significantly lower extent, probably due to the anti-cooperativity arising from unfavorable electrostatic interactions.

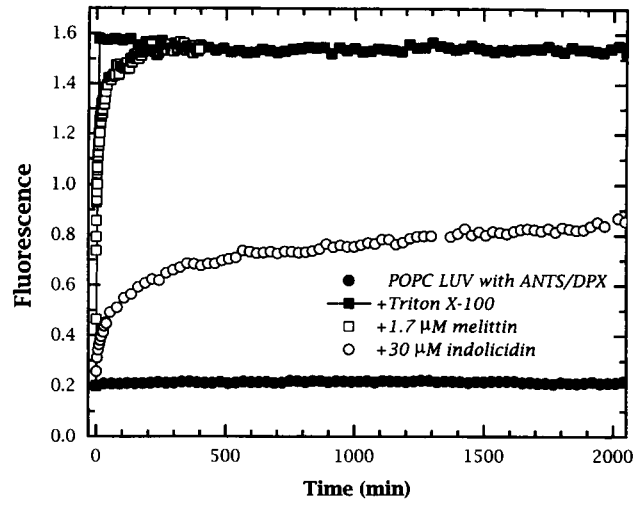

FIGURE 2 Fluorescence of ANTS/DPX-loaded POPC LUV (0.6 mM lipid) in the absence and presence of leakage-inducing agents. Leakage of contents leads to a dilution of quencher (*DPX*) around the dye molecule (*ANTS*) and thereby increases fluorescence. POPC vesicles containing ANTS/DPX (●) in the absence of disrupting agents show a stable fluorescence signal. Disruption of vesicles with Triton X-100 (■) causes maximal fluorescence increase. The lytic peptide melittin (□) causes rapid and complete release of ANTS/DPX as indicated by the fluorescence increase that is the same as for Triton X-100. Indolicidin (○), even at the very high concentration used here, does not lead to the complete release of markers even after several hours of incubation.

Indolicidin-induced leakage of vesicle contents

Lipid dependence of leakage rates from DPX/ANTS-loaded vesicles

The release of the contents of ANTS/DPX-loaded vesicles induced by indolicidin was monitored by following the increase in fluorescence as illustrated in Fig. 2 for POPC LUV. The release in this case is very slow; the fluorescence increase does not reach the level obtained following disruption with Triton X-100 even many hours after mixing with high indolicidin concentrations. Although the extrusion technique is known to produce homogeneous unilamellar vesicles (Mui et al., 1993; Mayer et al., 1986), such a result could occur if the vesicle preparation had been contaminated with high amounts of multilamellar vesicles. To exclude such a possibility, we compared the action of indolicidin with that of the peptide melittin, which causes fast and complete leakage of vesicle contents at low concentrations without causing fusion or micellization (Benachir and Lafleur, 1995; Schwarz et al., 1992). We see complete release (Fig. 2) at a melittin/lipid ratio of 0.3%,which is well below the ratios at which micellization (~5%) or fusion (>0.5%) occur [see review by Dempsey (1990)]. Melittin also causes complete leakage of the contents of POPG vesicles (data not shown). Because the melittin-induced leakage involves pore formation or membrane perturbations of some sort that should also be affected by significant populations of multi-lamellar vesicles, we conclude that our vesicles are unilamellar.

The indolicidin-induced leakage from anionic POPG vesicles is very fast and effective (Fig. 3). The same concentration of indolicidin (30 μM), that caused only one-third of the total fractional fluorescence change for POPC vesicles in 30 min, caused maximum possible fluorescence increase

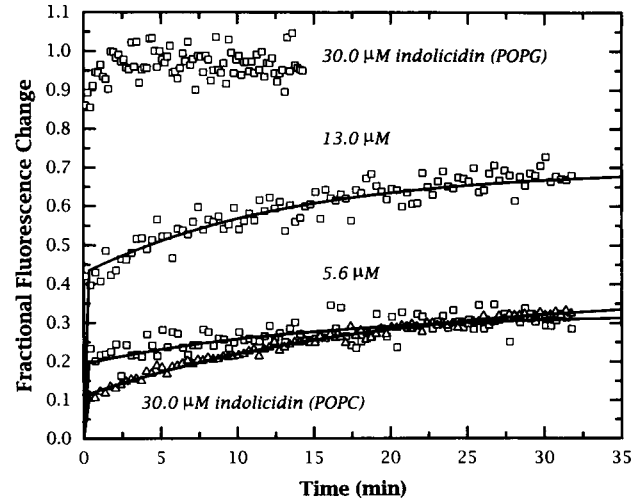

FIGURE 3 Normalized fluorescence increase of ANTS/DPX-loaded POPG (□) and POPC (△) LUV (0.6 mM lipid) after the addition of indolicidin at the concentrations indicated on the figure. To allow a better comparison, the fluorescence increase of ANTS is normalized so that the absence of leakage corresponds to 0 and the fluorescence increase observed with Triton X-100 corresponds to 1. Curves through the points correspond to fit with Eq. 6 in combination with Eq. A1. Parameters of the fits are presented in Table 2. The leakage caused by indolicidin from anionic POPG vesicles is more effective than from neutral POPC vesicles.

of POPG LUV in 3 min. Such a significant qualitative difference in dose-response dependence strongly suggests a difference in the structural organization of indolicidin complexed with neutral and anionic bilayers. No significant fusion of vesicles could be detected at the indolicidin concentrations used. A quantitative analysis of the kinetics, which requires a prior determination of mechanism of leakage, is presented below.

Determination of the mechanisms of leakage

The fluorescence requenching technique was used to establish the nature of the leakage induced by indolicidin (Ladokhin et al., 1995; Wimley et al., 1994). The internal quenching (Q_{in}) as a function of ANTS released (f_{out}) that results from the action of indolicidin on POPC and POPG LUV is presented in Fig. 4. To distinguish among the possible mechanisms of leakage, two "landmarks" are established in each case. The first landmark, shown by the dashed line labeled AON, represents all-or-none leakage for which Q_{in} is independent of f_{out} and is established by simply passing a horizontal line through the value of Q_{in} for f_{out} = 0. The second landmark, shown by the dotted curve labeled GNP, represents graded nonpreferential release of ANTS/DPX. This curve is established using Eq. 4 with $\alpha = 1$ and a value of $[DPX]_0$ chosen to make Q_{in} equal the value observed for $f_{out} = 0$. We note that the trapping efficiency of vesicles for DPX depends strongly on lipid composition as indicated by the different values of $[DPX]_0$ for POPG and POPC vesicles (Fig. 4, legend).

The two lipid systems clearly exhibit very different behaviors relative to the GNP and AON landmarks. For POPG, Q_{in} increases strongly with f_{out} and thereby indicates graded release. Because all values of Q_{in} are substantially above the dotted GNP reference line, the leakage is selective for DPX. For POPC, Q_{in} depends weakly, if at all, on f_{out} and could be due to one of several mechanisms, as discussed below. The selectivity of the graded leakage from POPG vesicles can be determined quantitatively by finding the value of α that gives the best nonlinear least-squares fit of Eq. 4 to the experimental values of Q_{in}. This procedure yields $\alpha = 3.1 \pm 0.4$, which means that the leakage path is highly selective for DPX. The plot of Eq. 4 obtained using this value of α is shown by the solid line labeled GPD in the POPG panel of Fig. 4.

As shown in the bottom panel of Fig. 4, release from POPC vesicles is consistent with several possibilities including all-or-none (*dashed line* labeled *AON*) and nonpreferential graded release (*dotted line* labeled *GNP*) as limiting cases. The area between the two curves can be explained by numerous possibilities that include graded preferential release of ANTS (with apparent $\alpha = 0.63$ determined by the best fit to Eq. 4, data not shown) or some combination of graded and all-or-none mechanisms (Ladokhin et al., 1995). In any case, the leakage from POPC vesicles is clearly not consistent with graded preferential DPX release (*solid line* labeled *GPD*) as observed for POPG vesicles.

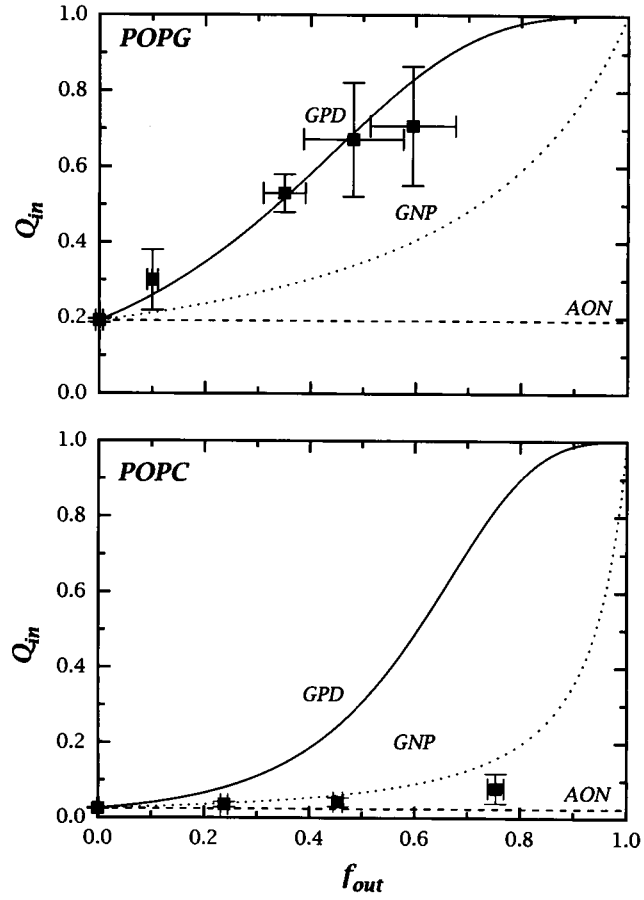

FIGURE 4 Plots of internal quenching (Q_{in}) of ANTS inside vesicles as a function of the ANTS released (f_{out}) by indolicidin from POPG and POPC vesicles. POPG: Solid curve (*GPD*) is the best fit to the data using Eq. 4 ($\alpha = 3.1 \pm 0.4$, $[DPX]_0 = 6.1 \pm 0.2$ mM) suggesting that release is graded with strong preferential leakage of DPX. The other two curves, also calculated using $[DPX]_0 = 6.1$, correspond to all-or-none release (*dashed curve, AON*) and graded non-preferential with $\alpha = 1$ (*dotted curve, GNP*). POPC: Dashed curve (*AON*) and dotted curve (*GNP*) correspond, respectively, to all-or-none and to graded nonpreferential release with $\alpha = 1$. The graded preferential release with $\alpha = 3.1$ is not consistent with the data (*solid curve, GPD*). $[DPX]_0 = 30$ mM in all cases. The requenching data do not allow unique assignment of mechanism of leakage for POPC. However, it is clear that the mechanism is different for anionic and neutral vesicles.

Kinetics of the indolicidin-induced leakage

Fluorescence kinetics do not follow the release-of-contents kinetics unless the release is all-or-none (Schwarz and Arbuzova, 1995; Ladokhin et al., 1995). The deviation between the kinetics depends strongly on the parameter of preferential release α and therefore should be significant for the ANTS/DPX efflux from POPG vesicles. The procedure that accounts for the kinetic difference for preferential release of either DPX or ANTS is described in detail in the Appendix. Briefly, the time-dependent fluorescence $F(t)$ is related to Q_{in} and to the efflux of dye f_{out} through Eq. A1, with $f_{out}(t)$ being described by the empirical multi-exponential release model (Eq. 6). The dependence of Q_{in} on α given by Eq. 4 allows one to account for the effects of graded

release on fluorescence kinetics. The results of nonlinear least-squares fits of Eqs. 6 and A1 to the fluorescence kinetics accompanying indolicidin-induced leakage are presented in Table 2 and Fig. 3. The effective parameters of leakage derived from the empirical kinetic parameters A_0, A_1, and k_1 and the parameter α (Eqs. A4–A6) indicate that the release of both markers from POPG LUV is faster and more efficient than release from POPC vesicles.

Spectroscopic characterization of free and membrane-bound indolicidin

Tryptophan absorbance and fluorescence

The near-UV absorbance spectrum of free or bound indolicidin was found to be equivalent to the superposition of its five tryptophan residues corresponding to a molar extinction coefficient of 28×10^3 M^{-1} cm^{-1} at 280 nm. In solution, indolicidin exhibits a fluorescence with maximum at 348 nm, characteristic of water-exposed tryptophans (Table 3; Fig. 5, *top*). The average quantum yield of the five tryptophan residues reaches only 38% of that of the tryptophan zwitterion in aqueous solution.

Consistent with the observations of Ahmad et al. (1995), the fluorescence of indolicidin is sensitive to membrane binding. The data of Table 3 and Fig. 5 show that indolicidin partitioning into bilayers leads to blue shifts of the spectra and increases in quantum yields. Compared with POPC, binding to POPG results in a greater spectral shift, but with lower quantum yield. Such differences could be due to differences in the structure of the indolicidin in the two membranes, a general effect of lipid type on the fluorescence of the indole fluorophore, or a combination of the two. To investigate these possibilities, we examined the effect of lipid composition on the fluorescence of the model compound TOE, which has proven useful for modeling tryptophan fluorescence in membranes (Ladokhin and Holloway, 1995b). TOE binds equally strongly to both POPC and POPG LUV with partition coefficients of 6.4 ± 0.7 10^6 (data not shown). The data in Table 3 and the bottom panel of Fig. 5 show that the fluorescence spectral changes of TOE parallel those of indolicidin. Furthermore, the quantum yield of POPG-bound TOE is smaller than POPC-bound TOE with the difference being even greater than for indolicidin. Therefore, regardless of the possible structural differences between POPC- and POPG-bound indolicidin, the fluorescence differences are influenced to a large extent by the effects of the membrane on the fluorophore itself. The cause of such generic effects is uncertain, but they might possibly be due to changes in the natural lifetime and/or quenching rates caused by differences in the chemical structures and hydration of the lipids.

TABLE 3 Fluorescence parameters of indolicidin (Ind) and the model compound, tryptophan octyl ester (TOE), in solution and when bound to POPC or POPG vesicles

	Quantum yield (rel. to free Trp)	Spectral maximum	Anisotropy	Fraction bound*
Indolicidin	38%	348 nm	0.032	
Ind + POPC	56%	338 nm	0.053	97%
Ind + POPG	47%	335 nm	0.060	100%
TOE	41%	350 nm	0.005	
TOE + POPC	78%	337 nm	0.086	99%
TOE + POPG	48%	335 nm	0.088	99%

*Fraction of bound molecules calculated from the equilibrium dialysis binding studies.

We performed fluorescence polarization measurements that are sensitive to both rotational movement and energy transfer between fluorophores. The membrane-bound indolicidin has a lower anisotropy than the much smaller TOE molecule (Table 3) suggesting that the fluorescence is partly depolarized by energy transfer occurring between some or all tryptophan residues. The difference in anisotropy between POPC- and POPG-bound indolicidin is insignificant.

We found that all of the fluorescence changes that occurred upon partitioning into either POPC or POPG LUV were complete by the time the data could be acquired (<1 min after mixing) and no further changes could be detected during prolonged incubations (up to 10 h). This indicates that the leakage kinetics (Fig. 3) are most likely due to the peculiarities of the structural rearrangements of peptide already bound to vesicles rather than to time-dependent binding of the peptide. Such rearrangements often do not result in measurable changes in intrinsic fluorescence unless some specific quenching technique is used (Ladokhin and Holloway, 1995a,b; Matsuzaki et al., 1995). Unfortunately, the probable existence of energy transfer between indolicidin's tryptophans precludes the application of such techniques to indolicidin.

TABLE 2 Kinetic parameters for the leakage of ANTS and DPX from POPC and POPG vesicles

Indolicidin concentration	Empirical kinetic parameters*			Effective parameters of leakage#		
+ Lipid (0.6 mM)	A_0	A_1	k_1 (10^{-3} sec^{-1})	$A^{ANTS}_{released}$ (% per μM)	$A^{DPX}_{released}$ (% per μM)	k_{eff} (10^{-3} sec^{-1})
30 μM + POPC	0.11	0.27	0.86	1.3	1.3	1.21
5.6 μM + POPG	0.11	0.07	1.06	3.3	8.5	2.64
13 μM + POPG	0.24	0.17	1.09	3.2	6.2	2.60

*Empirical kinetic parameters were recovered by fitting fluorescence kinetics data from Fig. 3 with Eq. 6 together with Eq. A1.
#Effective parameters of leakage are calculated from kinetic parameters and parameters of preferential release, α, according to Eqs. A4–A6.

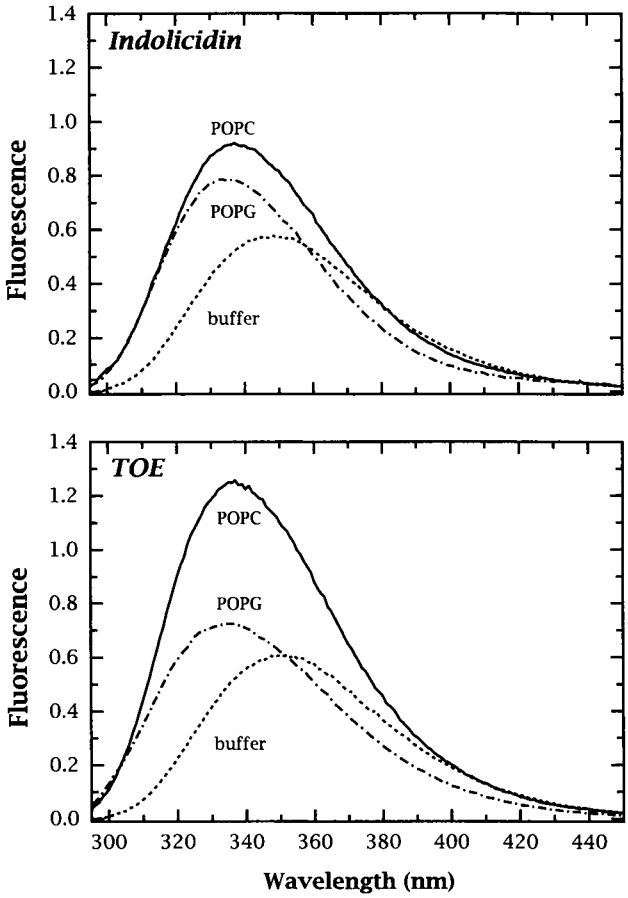

FIGURE 5 Fluorescence of indolicidin and the model tryptophan derivative TOE in buffer and bound to POPC and POPG LUV. The fluorescence of indolicidin is sensitive to whether it binds to neutral or anionic membranes. However, changes in TOE fluorescence are similar to those of indolicidin (see also Table 3). This leads to the conclusion that regardless of the possible structural differences between POPC- and POPG-bound indolicidin, the difference in their fluorescence is strongly influenced by lipid headgroup effects on the fluorophore itself.

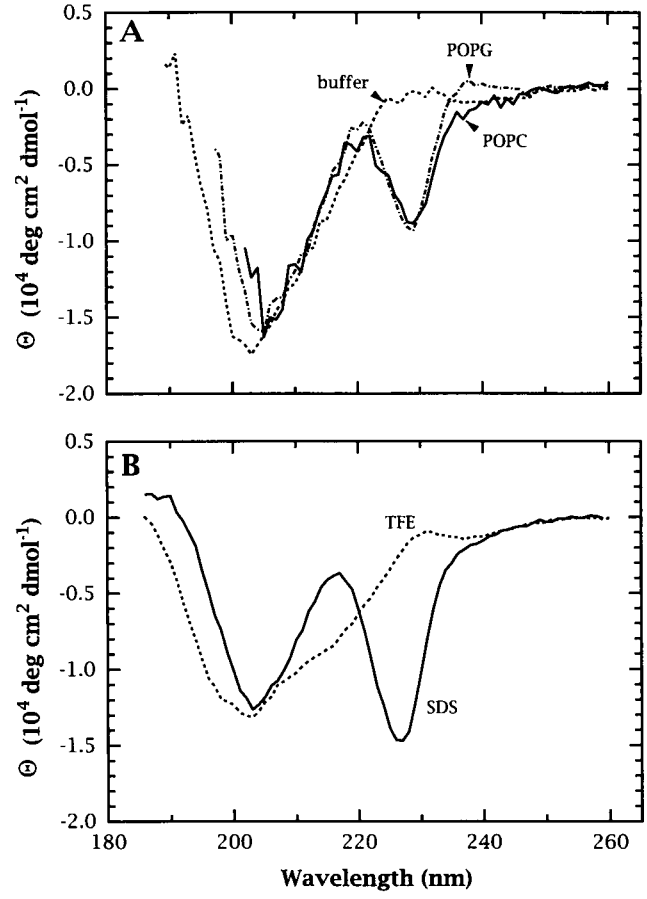

FIGURE 6 CD spectrum of indolicidin in (*A*) aqueous buffer, POPC bilayers, and POPG bilayers, and (*B*) in two model systems used to emulate membrane environments. (*A*) CD spectra for indolicidin in buffer, POPC, and POPG are indicated on the figure. Expressed as a per residue ellipticity, all CD spectra are consistent with unordered backbone structures. The negative bands seen in the POPG and POPC spectra are due to tryptophan, and are commonly observed in tryptophan-containing peptides that are partitioned into bilayers (see text). The narrowing of the negative 200-nm band in the bilayer spectra suggests that the conformational states available to indolicidin are restricted compared to aqueous buffer. (*B*) CD spectra of indolicidin in trifluoroethanol (TFE) and 10 mM SDS micelles are indicated in the figure. Indolicidin in TFE has a spectrum similar to that observed in aqueous buffer. Notice that the SDS spectrum shows a strong negative band at 230 nm similar to, but stronger than, the one observed for POPC and POPG. Also notice that the negative band at 200 nm is narrower in the SDS spectrum which, as for the POPC and POPG spectra in (*A*), suggests restriction of conformational states.

Circular dichroism spectroscopy

The far-UV CD spectrum of indolicidin in aqueous buffer and in trifluoroethanol (Fig. 6) or methanol (data not shown) is characterized by a minimum at 200 nm that is usually considered characteristic of an unordered backbone structure (Park et al., 1992; Perczel et al., 1991; Brahms and Brahms, 1980). However, the low ellipticity of the peak resembles the signal from peptides containing a β-turn (Blanco et al., 1994; Sieber and Moe, 1996). The near-UV CD spectrum (not shown) contains relatively small negative peaks corresponding to L_a, L_b (270–290 nm) and, probably, B_b (240 nm) transitions of the indole chromophore.

Addition of the highly scattering vesicles impaired our ability to measure CD spectra at wavelengths shorter than 195 nm. Nevertheless, upon membrane partitioning, we can detect changes in the position of the main band and also the appearance of an extra negative peak at ~230 nm (Fig. 6 *A*). Although we cannot rule out entirely a change in backbone conformation as an explanation of the new band, it is very probably due to changes in the tryptophans' environment as suggested by model studies and calculations discussed by Woody (1994) and studies of gramicidins (Woolley et al., 1992; Sawyer et al., 1990). Furthermore, membrane-bound tryptophan-containing short peptides show a similar peak (data not shown). A similar negative peak is also present in the CD spectrum of indolicidin bound to SDS micelles (Fig. 6 *B*). For that case, the differences observed at shorter wavelengths are even more pronounced compared with the vesicle-bound form, suggesting additional changes in the backbone structure. The spectrum in SDS was found to be

independent of indolicidin concentration, at least between 0.5 and 50 μM, indicating that aggregation is unlikely to be involved. Because of the strong tryptophan contribution and the absence of standard spectra for short peptides in membrane environments, we did not attempt to deconvolute the CD spectra of indolicidin into individual components representing different types of secondary structures.

DISCUSSION

Disposition of indolicidin in POPC and POPG bilayers

Indolicidin partitions strongly, but reversibly, into both neutral POPC and anionic POPG bilayers as determined by equilibrium dialysis measurements (Fig. 1). Ahmad et al. (1995) also concluded that indolicidin partitions strongly into POPC bilayers. The calculated free energies of transfer are $\Delta G = -8.8 \pm 0.2$ kcal/mol for POPC and -11.5 ± 0.4 kcal/mol for POPG LUV. These numbers are obtained under the assumption that both leaflets are accessible to indolicidin. If only the outer leaflets participate in binding, the values for free energies should be increased by 0.41 kcal/mol (see Methods). There is presently no unambiguous method for establishing the transbilayer distribution of bound peptides. We make the assumption that indolicidin is distributed equally across the membrane, since membrane permeabilization is consistent with significant perturbation of both leaflets.

The partitioning into POPG is so strong that a new method of determining partition coefficients was developed that involves measuring partitioning relative to POPC LUV rather than to buffer (see Materials and Methods). This approach broadens the range of partition coefficient values that can be determined by equilibrium dialysis methods.

The partitioning of indolicidin into neutral POPC vesicles is probably driven primarily by the hydrophobic effect operating on the five tryptophans (Wimley and White, 1996). Electrostatic interactions among indolicidin's four basic groups (one Lys, two Arg, and the amino terminus), on the other hand, may dominate binding to POPG vesicles. This possibility can be examined through calculations of electrostatic binding using the equations of Ben-Tal et al. (1996). Assuming only electrostatic (ES) interactions, we calculate $\Delta G_{ES} = -10.2$ kcal/mol using mole-fraction units and our experimental conditions. Thus, electrostatic interactions can account for most, but not all, of the transfer free energy into POPG. Presumably hydrophobic interactions occur in addition, but to conclude that the difference of -1.3 kcal/mol represents the full extent of the hydrophobic contribution would be premature because the behavior of a charged hydrophobic peptide at the POPG interface is likely to be more complex than assumed in the Ben-Tal et al. (1996) model for binding. The model specifically assumes that the peptides do not penetrate the polar headgroup region. Ben-Tal et al.'s experimental measurements using hydrophilic Lys peptides were entirely consistent with that assumption. For peptides such as indolicidin that are rich in both charged and hydrophobic residues, one can reasonably assume that the disposition of the peptides in the bilayer interface is much more complex. One can easily imagine a compromise structural arrangement such that neither hydrophobic nor electrostatic interactions are expressed fully. Studies of synthetic variants of indolicidin may allow the relative contributions of hydrophobic and electrostatic interactions under various conditions to be sorted out.

CD and fluorescence spectroscopy measurements of indolicidin bound to both POPC and POPG bilayers are generally consistent with a largely unordered backbone conformation of indolicidin located in the interfacial regions. The CD measurements indicate that indolicidin adopts an unordered conformation in POPC and POPG vesicles as well as in isotropic homogeneous solvents based upon a characteristic minimum at ~200 nm (Fig. 6). However, the per-residue ellipticity is much smaller than reported for random-coil peptides (Brahms and Brahms, 1980) or unordered conformations of water-soluble (Perczel et al., 1991) and membrane proteins (Park et al., 1992). The reduced ellipticity may be due to contributions from the tryptophans which are especially abundant in indolicidin and are expected to have higher contribution in peptides with lower helical content (Woody, 1994). In several recent publications a similarly shaped spectrum with low per-residue ellipticity was reported for peptides containing a β-hairpin structure as determined by NMR (Sieber and Moe, 1996; Blanco et al., 1994). Falla et al. (1996) have observed CD spectra similar to ours for an indolicidin-like compound (indolicidin without the C-terminus amide) bound to bilayers and concluded that polyproline II helices are formed. The characteristic features of polyproline II helices are a negative peak at ~205 nm and a positive peak at ~230 nm (Ronish and Krimm, 1974). Although our negative peak at ~200 nm represents a shift to longer wavelengths relative to the expected value of 197 nm for pure random coil, we suggest that this evidence alone does not support the existence of polyproline II helices; such a shift could be due to other conformations (e.g., β-hairpins). In any case, there is certainly no α-helical structure because of the complete absence of characteristic minima at 208 and 222 nm. An important feature of the CD spectra of indolicidin bound to both POPC and POPG membranes, that is also observed for indolicidin in SDS micelles, is a strong negative peak at 230 nm that is characteristic of tryptophan-containing peptides that partition into bilayers without forming α-helices (Woolley et al., 1992; Sawyer et al., 1990). This negative peak makes it impossible to observe a positive peak at 230 nm due to polyproline II helices, if they exist.

The fluorescence measurements indicate that indolicidin's five tryptophans are sensitive to membrane binding as indicated by an increased quantum yield and a blue-shifted spectrum (Fig. 5, *top*; Table 3). Such changes are generally observed when tryptophan is transferred into an environment that is less polar or motionally more restricted than water. Binding to POPG causes a greater spectral shift, but

smaller intensity increase, compared with binding to POPC. A similar pattern was reported for fluorescence changes in melittin upon binding to neutral and anionic lipids (Dufourcq and Faucon, 1977). However, these differences do not necessarily indicate differences in membrane location of indolicidin or melittin because similar differences are observed for TOE (Fig. 5, *bottom*; Table 3) whose "structure" in the two types of vesicles is expected to be very similar. Whatever the explanation is for the difference in fluorescence properties between POPC- and POPG-bound indolicidin, the difference appears to arise primarily from the influence of the lipid environment on the indole chromophore rather than from differences in peptide conformation.

Existence of the radiationless energy transfer between the tryptophans of indolicidin results in lower polarization of the fluorescence as compared with a model compound TOE (Table 3) and impairs our ability to use such measurements for structural studies. Nevertheless, the positions of the spectra of membrane-bound indolicidin and membrane-bound TOE are very similar. This indicates that emitting tryptophans in indolicidin are located in an environment similar to that of the tryptophan of TOE whose transverse distance from bilayer center in neutral lipids is ~11 Å (Ladokhin and Holloway, 1995b).

Indolicidin-induced leakage of vesicle contents

Our data demonstrate that indolicidin causes leakage of the contents of LUV loaded with the fluorophore/quencher pair ANTS/DPX (Figs. 2 and 3), consistent with the hypothesis that its in vitro antimicrobial action is related to membrane permeabilization. We found that indolicidin is much more efficient against anionic POPG LUV than against neutral POPC LUV. Ahmad et al. (1995) found hemolytic activity at relatively high indolicidin concentrations that was correlated with its aggregation in buffer. We restricted our attention to comparatively low concentrations of indolicidin (<30 μM) to characterize its behavior in the monomeric state. Our results indicate that monomeric indolicidin can cause significant, if not complete, release of contents of POPG LUV. Multimeric indolicidin will presumably act differently.

One of the principal problems of leakage studies is the determination of the mechanism by which release occurs. Generally, leakage can be a graded process in which all of the vesicles release portions of their contents, or it can be all-or-none, in which different populations of vesicles either lose all of their contents or lose none. Our results clearly demonstrate that for anionic vesicles formed with POPG, the leakage occurs via a graded mechanism with a high preference for the release of DPX over ANTS (Fig. 4 *A*). For neutral POPC vesicles, the ANTS/DPX requenching data are ambiguous (Fig. 4 *B*) because the requenching technique does not allow all-or-none release to be distinguished from preferential release of ANTS in the present case (Ladokhin et al., 1995). However, it is quite clear that release from POPC is not characterized by a preference for DPX. There is a possibility that, unlike for POPG, an all-or-none mechanism contributes to the release of ANTS/DPX from POPC.

The kinetics of leakage caused by indolicidin are complex and depend on the type of lipid used in the formation of the vesicles. An empirical kinetic model for multi-exponential release (Eq. 6) can be used to quantitate the time-dependent fluorescent changes and to convert them into the effluxes of ANTS and DPX (see also Appendix). The three parameters of the model quantitate the fraction of dye that is released immediately (A_0), the subsequent fraction of dye released with the measurable rate (A_1), and the rate with which the latter fraction is released (k_1). These parameters can be used to define three independent measures of overall effectiveness of leakage (Appendix, Eqs. A4–A6) which, when combined with results of the requenching analysis, permit a good assessment of leakage effectiveness. The measures include the amount of ANTS released per unit of peptide concentration, the concentration-normalized amount of DPX released, and the effective rate of dye release.

Application of these measures to our data shows that anionic POPG vesicles are induced to release more of both cationic DPX and anionic ANTS and to do it at a higher rate than POPC vesicles (Table 2). This could be related to the difference in the organization of the leakage pathway in two lipid systems. The observation that graded release of ANTS/DPX caused by indolicidin in POPG is more effective than possible all-or-none release in POPC is not surprising when considered in the context of the behavior human neutrophil defensin peptide HNP-2 that has a compact β-sheet structure stabilized by three disulfide bonds [see review by White et al. (1995)]. Reduced and denatured HNP-2 causes more effective release via a graded mechanism than native HNP-2 does via an all-or-none mechanism (Wimley et al., 1994). One can speculate that formation of a stable structured leakage path that causes all-or-none release may require more peptide than a fluctuational destabilization of a bilayer presumed to be responsible for graded release.

Use of indolicidin variants for studies of peptide-bilayer interactions

We suggested in the introduction to this paper that indolicidin is a useful starting peptide for general studies of peptide-bilayer interactions. Although one can in principle design peptides de novo to examine such things as relative contributions of hydrophobic and electrostatic interactions, a more economical approach is to begin with a natural peptide whose physical behavior is commensurate with the design objectives. In addition to the obvious objectives of good aqueous solubility and membrane partitioning, a particularly important objective for our work is lack of secondary structure in the bound and free states. This is essential for the first step of understanding the energetics of secondary

structure formation in peptides bound to bilayers, and more generally for protein folding in membranes (Wimley and White, 1996). The 26-residue bee venom peptide melittin, for example, partitions strongly into neutral and charged bilayers as an amphipathic helix, whereas in the free state it is largely unordered (Vogel, 1981). To quantitate the energetics of helix formation, one must be able to calculate the free energy of transfer of melittin in the unfolded form, because the energetics of folding are revealed by the difference in the free energy of partitioning the folded and unfolded peptide. In their simplest form, such calculations require linearly additive and sequence-position independent free-energy-of-transfer scales for single amino acid residues that account for both hydrophobic and electrostatic interactions. Wimley and White (1996) have recently published a POPC-based interfacial "hydrophobicity" scale for this purpose derived from partitioning studies of pentapeptides. Some important next steps are to test the additivity of the scale for larger peptides and to sort out the relative contributions of hydrophobic, electrostatic, and bilayer-effect contributions to partitioning (White and Wimley, 1994).

We have demonstrated in this paper that indolicidin is largely unordered in both the bilayer-bound and free forms and that it interacts strongly with both neutral and cationic membranes. Indolicidin's five tryptophans provide a unique opportunity to examine the role of tryptophan in the insertion of proteins into membranes (Wimley and White, 1993a) and we have found that indolicidin variants are easy to synthesize without compromising solubility. Thus, indolicidin's amino acid sequence appears to be an ideal one to use as a starting point for understanding the interactions of unfolded peptides with lipid bilayers.

APPENDIX

Kinetic model of leakage

The relation between fluorescence changes, F, and the fraction of dye which is released, f_{out}, as a function of the time t that elapsed after mixing of marker-loaded vesicles with leakage-inducing agent, is described by (Ladokhin et al., 1995)

$$F(t) = F^{max} \times \{f_{out}(t) + Q_{in}(t) \cdot [1 - f_{out}(t)]\} \quad (A1)$$

where F^{max} is the maximal fluorescence observed when vesicles are disrupted with Triton X-100. Q_{in} is independent of f_{out} for all-or-none release or described by Eq. 4 when release is graded. Equation A1 can be used for fitting experimental data only when a kinetic model of leakage that describes the time dependence of $f_{out}(t)$ is introduced. For that purpose, we utilize an empirical multi-exponential release model:

$$f_{out}(t) = 1 - \sum A_i \cdot \exp(-k_i t) \quad (A2)$$

where $\Sigma A_i = 1$. For simplicity, we assume that only three components are present in the sum and that one of them has an infinitely high rate ($k_0 = \infty$; in computations the value of $10^6\ s^{-1}$ was used) and another component has a zero rate ($k_2 = 0$). Because of these choices, only three independent parameters are necessary: the fraction A_0 that can be released immediately, the fraction A_1 that can be released with a measurable rate, and the rate itself (k_1). These choices simplify Eq. A2 to

$$f_{out}(t) = A_0 + A_1 \cdot [1 - \exp(-k_1 t)] \quad (A3)$$

The three parameters of this equation can be obtained by fitting the experimentally observed fluorescence kinetics to Eq. A1 after substituting Q_{in} obtained from Eq. 4, and f_{out} obtained from Eq. A2, or its simplified form Eq. A3. First, however, the mechanism of release must be established and, in case of graded release, the value of α must be estimated by the fluorescence requenching method by means of Eq. 4 (Ladokhin et al., 1995). Once this is accomplished, the overall effectiveness of leakage of ANTS and DPX can be characterized separately. For that purpose, three independent measures that utilize both kinetic and requenching data can be used as follows.

1. *Effectiveness of ANTS leakage* is characterized by the ratio of the amount of ANTS that can be released according to Eq. 6 to the concentration of the bound peptide:

$$A^{ANTS}_{released} = \frac{f_{out}(\infty)}{[Peptide]} = \frac{A_0 + A_1}{[Peptide]} \quad (A4)$$

2. *Effectiveness of DPX leakage* is characterized by the ratio of the amount of DPX that can be released according to Eq. 5 to the concentration of the bound peptide which for all-or-none release coincides with the effectiveness of ANTS leakage. For graded release

$$A^{DPX}_{released} = \frac{1 - (1 - f_{out}(\infty))^{\alpha}}{[Peptide]} = \frac{1 - (1 - A_0 - A_1)^{\alpha}}{[Peptide]} \quad (A5)$$

3. *The effective rate of ANTS leakage* is a reciprocal of an A-weighted average correlation time of the release of the portion of ANTS that can be released according to Eq. A3:

$$k_{eff} = \left[\frac{(A_0/k_0) + (A_1/k_1)}{A_0 + A_1}\right]^{-1} = \frac{A_0 + A_1}{A_1} \cdot k_1 \quad (A6)$$

Note that the effective rate of DPX leakage is not truly an independent parameter because the kinetics of DPX are related to the kinetics of ANTS (Eq. 5).

We chose the multi-exponential release model because of its apparent simplicity (only three fitting parameters are sufficient to get an adequate fit as shown in Fig. 3) and because it does not require the assumption that the contents are fully released at infinite time. That assumption is utilized in the widely used model of Schwarz and co-workers (Schwarz and Robert, 1992; Schwarz and Arbuzova, 1995; Schwarz et al., 1992) but apparently is not valid in the case of indolicidin (see Fig. 2). Furthermore, the multi-exponential release model covers the situation of rapid equilibrium between free peptide and different forms of bound peptide that might each cause leakage with different rates as for magainin 2a (Grant et al., 1992).

We thank Dr. W. C. Wimley for technical assistance and helpful discussions. We are grateful to Dr. E. Habermann for the gift of the melittin and to Drs. N. Ben-Tal and S. McLaughlin for providing us with a copy of their manuscript, before publication, concerned with the electrostatic binding of peptides to charged bilayers. We thank the anonymous referees for their helpful remarks.

This research was supported by Grants GM-46823 (to S.H.W.) and AI-22931 (to M.E.S.) from the National Institutes of Health.

REFERENCES

Ahmad, I., W. R. Perkins, D. M. Lupan, M. E. Selsted, and A. S. Janoff. 1995. Liposomal entrapment of the neutrophil-derived peptide indolicidin endows it with in vivo antifungal activity. *Biochim. Biophys. Acta.* 1237:109–114.

Ben-Tal, N., B. Honig, R. M. Peitzsch, G. Denisov, and S. McLaughlin. 1996. Binding of small basic peptides to membranes containing acidic lipids: theoretical models and experimental results. *Biophys. J.* 71: 561–575.

Benachir, T., and M. Lafleur. 1995. Study of vesicle leakage induced by melittin. *Biochim. Biophys. Acta.* 1235:452–460.

Blanco, F. J., G. Rivas, and L. Serrano. 1994. A short linear peptide that folds into a native stable β-hairpin in aqueous solution. *Nat. Struct. Biol.* 1:584–590.

Brahms, S., and J. Brahms. 1980. Determination of protein secondary structure in solution by vacuum ultraviolet circular dichroism. *J. Mol. Biol.* 138:149–178.

Dempsey, C. E. 1990. The actions of melittin on membranes. *Biochim. Biophys. Acta.* 1031:143–161.

Dufourcq, J., and J. F. Faucon. 1977. Intrinsic fluorescence study of lipid-protein interactions in membrane models. Binding of melittin, an amphipathic peptide, to phospholipid vesicles. *Biochim. Biophys. Acta.* 467:1–11.

Falla, T. J., D. N. Karunaratne, and R. E. W. Hancock. 1996. Mode of action of the antimicrobial peptide indolicidin. *J. Biol. Chem.* 271: 19298–19303.

Grant, E., T. J. Beeler, K. M. P. Taylor, K. Gable, and M. A. Roseman. 1992. Mechanism of magainin-2a induced permeabilization of phospholipid vesicles. *Biochemistry.* 31:9912–9918.

Ladokhin, A. S., and P. W. Holloway. 1995a. Fluorescence quenching study of melittin-membrane interactions. *Ukr. Biokhim. Zh.* 67:34–40.

Ladokhin, A. S., and P. W. Holloway. 1995b. Fluorescence of membrane-bound tryptophan octyl ester: a model for studying intrinsic fluorescence of protein-membrane interactions. *Biophys. J.* 69:506–517.

Ladokhin, A. S., M. E. Selsted, and S. H. White. 1996. Interaction of antimicrobial peptide indolicidin with membranes. *Biophys. J.* 70:447*a* (Abstr.).

Ladokhin, A. S., L. Wang, A. W. Steggles, and P. W. Holloway. 1991. Fluorescence study of a mutant cytochrome b_5 with a single tryptophan in the membrane-binding domain. *Biochemistry.* 30:10200–10206.

Ladokhin, A. S., W. C. Wimley, and S. H. White. 1995. Leakage of membrane vesicle contents: determination of mechanism using fluorescence requenching. *Biophys. J.* 69:1964–1971.

Matsuzaki, K., O. Murase, N. Fujii, and K. Miyajima. 1995. Translocation of a channel-forming antimicrobial peptide, magainin 2, across lipid bilayers by forming a pore. *Biochemistry.* 34:6521–6526.

Mayer, L. D., M. J. Hope, and P. R. Cullis. 1986. Vesicles of variable sizes produced by a rapid extrusion procedure. *Biochim. Biophys. Acta.* 858: 161–168.

Mui, B. L.-S., P. R. Cullis, E. A. Evans, and T. D. Madden. 1993. Osmotic properties of large unilamellar vesicles prepared by extrusion. *Biophys. J.* 64:443–453.

Park, K., A. Perczel, and G. D. Fasman. 1992. Differentiation between transmembrane helices and peripheral helices by the deconvolution of circular dichroism spectra of membrane proteins. *Protein Sci.* 1:1032–1049.

Perczel, A., M. Hollosi, G. Tusnady, and G. D. Fasman. 1991. Convex constraint analysis: a natural deconvolution of circular dichroism curves of proteins. *Protein Eng.* 4:669–679.

Ronish, E. W., and S. Krimm. 1974. The calculated circular dichromism of polyproline II in the polarizabiliity approximation. *Biopolymers.* 13: 1635–1651.

Sawyer, D. B., L. P. Williams, W. L. Whaley, R. E. Koeppe, and O. S. Andersen. 1990. Gramicidins A, B, and C form structurally equivalent ion channels. *Biophys. J.* 58:1207–1212.

Schiffer, M., C. H. Chang, and F. J. Stevens. 1992. The functions of tryptophan residues in membrane proteins. *Protein Eng.* 5:213–214.

Schwarz, G., and A. Arbuzova. 1995. Pore kinetics reflected in the dequenching of a lipid vesicle entrapped fluorescent dye. *Biochim. Biophys. Acta.* 1239:51–57.

Schwarz, G., and C. H. Robert. 1992. Kinetics of pore-mediated release of marker molecules from liposomes or cells. *Biophys. Chem.* 42:291–296.

Schwarz, G., R. T. Zong, and T. Popescu. 1992. Kinetics of melittin induced pore formation in the membrane of lipid vesicles. *Biochim. Biophys. Acta.* 1110:97–104.

Selsted, M. E., M. J. Novotny, W. L. Morris, Y.-Q. Tang, W. Smith, and J. S. Cullor. 1992. Indolicidin, a novel bactericidal tridecapeptide amide from neutrophils. *J. Biol. Chem.* 267:4292–4295.

Sessa, G., J. H. Freer, G. Colacicco, and G. Weismann. 1969. Interaction of a lytic polypeptide, melittin, with lipid membrane systems. *J. Biol. Chem.* 244:3575–3582.

Sieber, V., and G. R. Moe. 1996. Interactions contributing to the formation of a β-hairpin-like structure in a small peptide. *Biochemistry.* 35: 181–188.

Van Abel, R. J., Y.-Q. Tang, V. S. V. Rao, C. H. Dobbs, D. Tran, G. Barany, and M. E. Selsted. 1995. Synthesis and characterization of indolicidin, a tryptophan-rich antimicrobial peptide from bovine neutrophils. *Int. J. Pept. Protein Res.* 45:401–409.

Vogel, H. 1981. Incorporation of melittin into phosphatidylcholine bilayers: study of binding and conformational changes. *FEBS Lett.* 134:37–42.

von Heijne, G. 1989. Control of topology and mode of assembly of a polytopic membrane protein by positively charged residues. *Nature (Lond.).* 341:456–458.

White, S. H., and W. C. Wimley. 1994. Peptides in lipid bilayers: structural and thermodynamic basis for partitioning and folding. *Curr. Opin. Struct. Biol.* 4:79–86.

White, S. H., W. C. Wimley, and M. E. Selsted. 1995. Structure, function, and membrane insertion of defensins. *Curr. Opin. Struct. Biol.* 5:521–527.

Williams, K. A., and C. M. Deber. 1991. Proline residues in transmembrane helices—structural or dynamic role? *Biochemistry.* 30: 8919–8923.

Wimley, W. C., M. E. Selsted, and S. H. White. 1994. Interactions between human defensins and lipid bilayers: evidence for the formation of multimeric pores. *Protein Sci.* 3:1362–1373.

Wimley, W. C., and S. H. White. 1993a. Membrane partitioning: distinguishing bilayer effects from the hydrophobic effect. *Biochemistry.* 32:6307–6312.

Wimley, W. C., and S. H. White. 1993b. Quantitation of electrostatic and hydrophobic membrane interactions by equilibrium dialysis and reverse-phase HPLC. *Anal. Biochem.* 213:213–217.

Wimley, W. C., and S. H. White. 1996. Experimentally determined hydrophobicity scale for proteins at membrane interfaces. *Nature Struct. Biol.* 3:842–848.

Woody, R. W. 1994. Contributions of tryptophan side chains to the far-ultraviolet circular dichroism of proteins. *Eur. Biophys. J.* 23: 253–262.

Woolley, G. A., A. Dunn, and B. A. Wallace. 1992. Gramicidin-lipid interactions induce specific tryptophan side-chain conformations. *Biochem. Soc. Trans.* 20:864–867.